Multi-Mode Smartphone Antenna Array for 5G Massive MIMO Applications

Naser Ojaroudi Parchin[*1], Haleh Jahanbakhsh Basherlou[2], Yasir I. A. Al-Yasir[1], Maryam Sajedin[3], Jonathan Rodriguez[3], and Raed A. Abd-Alhameed[1]

[1] Faculty of Engineering and Informatics, University of Bradford, Bradford BD7 1DP, UK
[2] Bradford College, Bradford, West Yorkshire, BD7 1AY, UK
[3] Instituto de Telecomunicações, Aveiro, Portugal
[*]N.OjaroudiParchin@Bradford.ac.uk

***Abstract* —A multi-band antenna array is proposed for 5G massive MIMO systems. The presented antenna not only exhibits multi-band operation but also generates the polarization diversity characteristic which makes it suitable for multi-mode operation. Its configuration contains eight modified planar-inverted F antenna (PIFA) elements located at different corners of the smartphone mainboard. For ease integration and design facilitation, the antenna elements and ground plane are etched on the same layer. For $S_{11} \leq -10$ dB, PIFA elements of the MIMO design operate at the frequency ranges of 2.5–2.7 GHz, 3.4–3.8 GHz, and 5.6–6 GHz covering the LTE 2600, 42/43, and 47 operation bands. Due to the placement of the antenna elements, the proposed design can support both vertical and horizontal polarizations. Fundamental characteristics of the proposed design are investigated. It offers good S-parameters, acceptable isolation, dual-polarized radiation coverage, and sufficient efficiency. In addition, the calculated TARC and ECC results of modified PIFAs are low over the operation bands.**

***Keywords* — 5G, multi-mode operation, massive MIMO, PIFA, smartphone applications.**

I. Introduction

The fifth-generation (5G) cellular communication has received great attention from both academia and industry with a lot of reported efforts [1-3]. 5G will have significant improvements in transmission rate, latency, mobility and so on. MIMO technology with multiple antennas is probably the most promising technology to reach the transfer data rates of 5G cellular communications. It can enhance channel capacity and link reliability of system [4-5]. The greater number of antennas can make it more resistant to intentional jamming and interference.

2 × 2 MIMO systems are successfully employed for 4G mobile networks and the massive MIMO system with a large number of antenna elements is expected to be applied for 5G communications [6-8]. Recently, several MIMO antenna designs have been introduced for 5G cellular systems [9-15]. However, all these mobile-phone antenna designs either exhibit single-band operation frequency or use a few antenna elements with large sizes which could occupy a huge space of smartphone mainboard. We propose here a new design of MIMO smartphone antenna with eight elements which unlike the reported designs can cover multi-frequency bands simultaneously. Modified PIFA elements are employed at four coroners of the PCB to operate at three different frequencies which makes the design more suitable for Massive MIMO communications. The PIFA is a popular and relatively low-profile antenna characterized by an omnidirectional radiation pattern [16-18]. Single-resonant, low-profile configuration of PIFAs suffer from impedance-bandwidth of multi-mode operation limitation [15].

The proposed MIMO PIFA system is designed to operate at three different bands including 2.6, 3.6, and 5.8 GHz of sub-6-GHz 5G cellular networks. The proposed MIMO system exhibits sufficient properties in terms of the fundamental antenna characteristics and could be used in future smartphones. The CST software is used to investigate the design properties [19]. The following sections present the antenna design details, single-element characteristics, and the performance of the proposed multi-band MIMO antenna.

II. Design Details of The Proposed Design

The configuration of the designed MIMO smartphone antenna is illustrated in Fig. 1. As shown, it is composed of four PIFA pairs that have been deployed at different corners of the mainboard. The proposed antenna is designed on the FR-4 dielectric with a thickness of h_x=1.6 mm. Each PIFA element is fed by a 50-Ohm discrete feeding technique extended from the ground plane to the antenna feedline. The parameter values of the design are listed in Table. I.

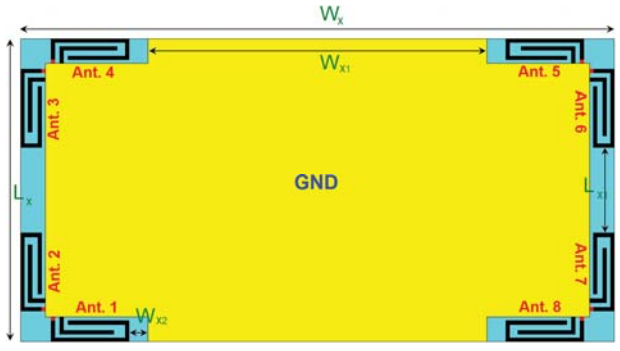

Fig. 1. The proposed Smartphone array antenna with modified PIFA elements.

TABLE. I VALUES OF THE DESIGN PARAMETERS

Parameter	W_X	L_X	W_{X1}	L_{X1}	W_{X2}	W	L	W_f
Value (mm)	150	75	83	18	5	20.5	6.5	1
Parameter	L_f	W_1	L_1	L_2	L_2	W_3	L_3	L_4
Value (mm)	1	1	15.3	3.5	14.3	16	5.5	4.5

III. PERFORMANCE OF THE ANTENNA ELEMENT

The configuration of the PIFA element is illustrated in Fig. 2 (a). Its structure is composed of an open-loop resonator with an L-shaped protruded strip. As shown, it has a compact size with a dimension of W×L. A 50 Ω discrete feeding port is employed to excite the antenna. The main motive behind the modified PIFA is to obtain a compact antenna element which can support different frequencies and could be integrated with a smartphone mainboard while occupying small clearance. Figure 2 (b) illustrates the simulated reflection coefficient (S_{11}) characteristic of the PIFA element. As shown, the antenna is operating at 2.6, 3.6, and 5.8 GHz with sufficient bandwidth and isolation characteristics.

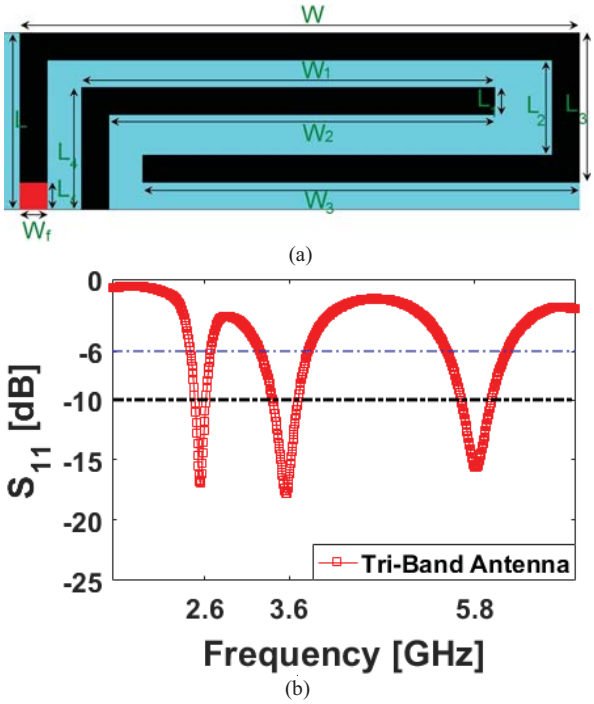

Fig. 2. (a) Transparent view of the PIFA antenna and (b) its S_{11} performance.

In order to justify the tri-band characteristic of the design, the simulated current densities of the modified PIFA element at different operation frequencies are illustrated in Fig. 3. It worth to mention that the maximum scaling for all figures is the same. At 2.6 GHz (first resonance), as can be seen, the L-shaped strip has a high current density with maximum current distribution. In addition, the current flow reverses on the interior edge of the surrounded open-loop. It is evident that the second resonance of the antenna S_{11} has been achieved using the open-loop resonator as it appears very active at 3.6 GHz. The third resonance can be considered as the second harmonic of the first resonance. As shown in Fig. 3 (c), the current distribution is almost equal around the L-shaped strip and the open-loop resonator. However, there is always some coupling between the employed square-ring slots, and the frequency response of the antenna is a result of these complex interactions [20-22]. The S_{11} characteristics of the modified PIFA antenna can be adjusted by changing the values for antenna parameters. Figure 4 illustrates the antenna S_{11} characteristic of varying design parameters including W_2, W_3, L_4, and W. As can be observed, the antenna frequency response in all operation bands is very flexible to be tuned to lower or upper frequencies. Its impedance matching can be also affected by changing the parameter values

Fig. 3. Surface Current densities at (a) 2.6 GHz, (b) 3.6 GHz, and (c) 5.8 GHz.

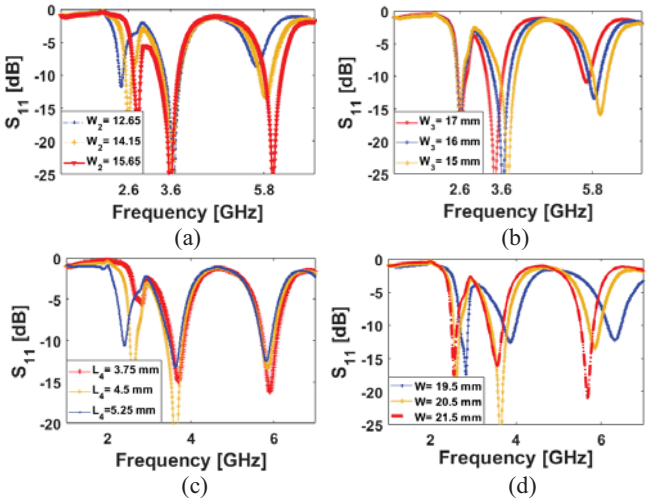

Fig. 4. The S_{11} results for different values of (a) W_2, (b) W_3, (c) L_4, and (d) W.

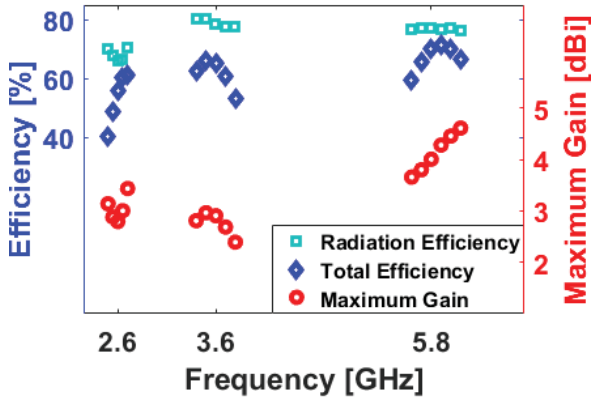

Fig. 5. Fundamental radiation characteristics versus the operation bands.

The fundamental radiation characteristics of the modified PIFA design including radiation efficiency (R.E.), total efficiency (T.E.) and maximum gain (M.G.) are represented in Fig. 5. As can be observed, the antenna provides sufficient efficiencies over the three operation band. In addition, the maximum gain of the design varies from 3 to 4.5 dBi.

IV. Characteristics of the Main Design

Figure 6 shows the S parameters (including S_{nn} and S_{mn}) of the designed smartphone antenna. As illustrated, the antenna exhibits good S parameters at three operation bands with acceptable mutual coupling less than -10 dB.

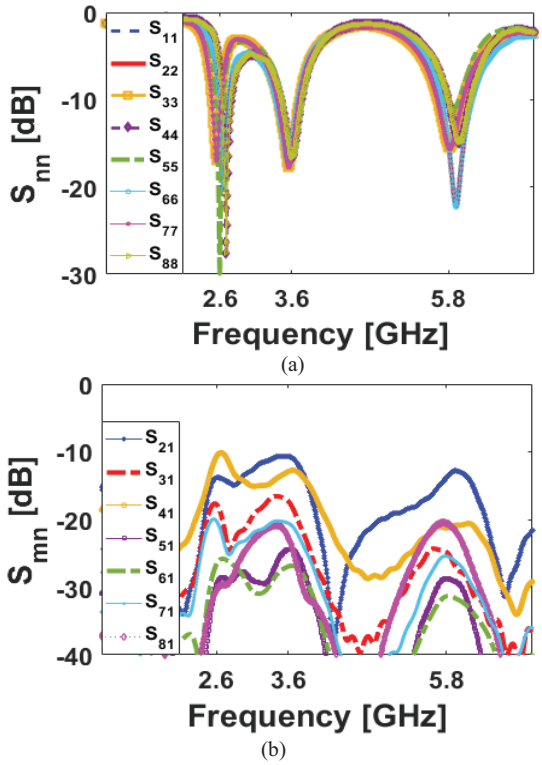

Fig. 6. (a) S_{nn} and (b) S_{mn} results of the proposed 5G smartphone antenna.

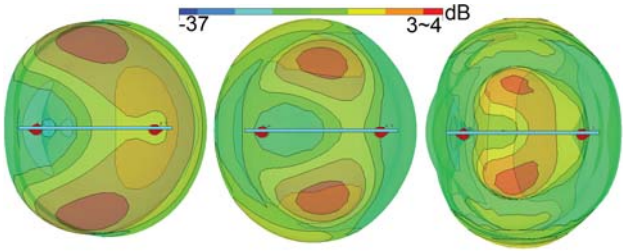

Fig. 7. Antenna radiation patterns at (a) 2.6 GHz, (b) 3.6 GHz, and (c) 5.8 GHz.

The side view of the design radiation patterns for a single-element radiator at different operation frequencies are shown in Fig. 7. Clearly, the antenna radiation elements provide high symmetric radiation patterns with covering the top/bottom sides of the mainboard and improving the radiation coverage [23-25].

The 3D radiation patterns for the eight PIFAs of the main design are displayed in Fig. 8. It can be observed that the 8-element MIMO antenna can offer sufficient gain vale for each radiator. As illustrated, the gain level of the design varies from 3 to more than 4 dBi. In addition, due to the placements of the PIFA element, four horizontally and vertically-polarized radiation patterns are achieved to improves the MIMO performance of the design [26-28].

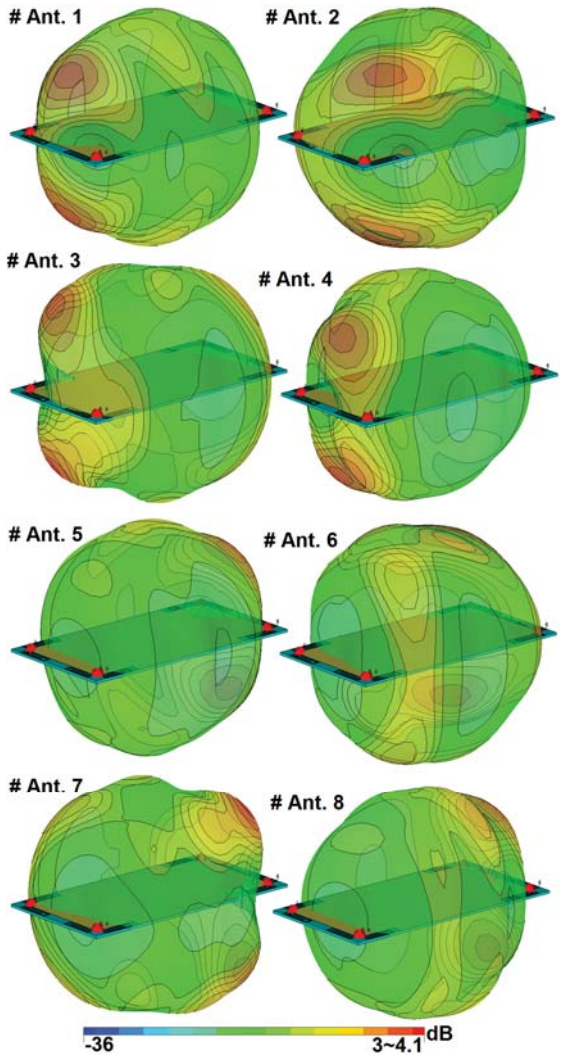

Fig. 8. Radiation patterns of the PIFAs at 3.6 GHz (middle frequency).

Total active reflection coefficient (TARC) and envelope correlation coefficient (ECC) characteristics are two important parameters to be considered in MIMO antennas [29-30]. The ECC and TARC characteristics of antenna pairs can be extracted from the S-parameter results using the below formulas, respectively.

$$ECC = \frac{|S_{mm}^{*}S_{nm}+S_{mn}^{*}S_{nn}|^{2}}{(1-|S_{mm}|^{2}-|S_{mn}|^{2})(1-|S_{nm}|^{2}-|S_{nn}|^{2})^{*}} \quad (1)$$

$$TARC = -\sqrt{\frac{(S_{mm}+S_{mn})^{2}+(S_{nm}+S_{nn})^{2}}{2}} \quad (2)$$

The ECC and TARC characteristics of the multi-mode smartphone MIMO antenna design are calculated and represented in Fig. 9. As evident from Fig. 9 (a), the calculated ECC results of PIFA pairs are very low entire the multi-operation bands (less than 0.01). In addition, as illustrated in Fig. 9 (b), the TARC value of the design is less than -20 dB at different frequencies.

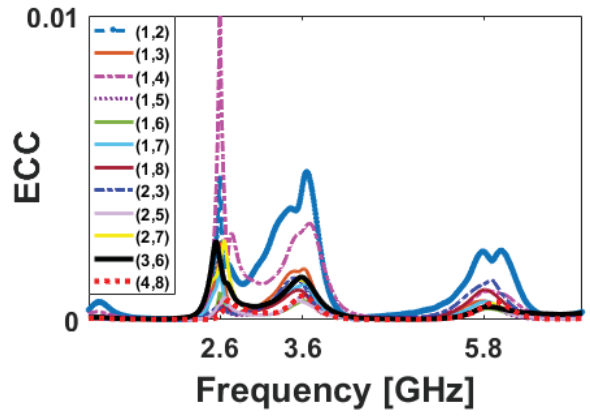

(a)

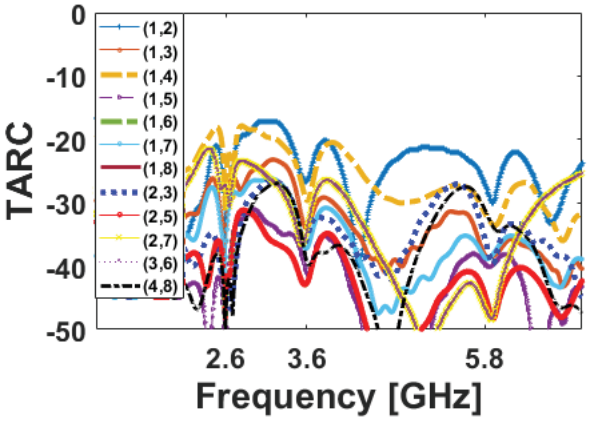

(b)

Fig. 9. Calculated (a) ECC and (b) TARC results of the proposed design.

V. Conclusion

Design and characteristics of a new tri-band MIMO antenna with dual-polarization function are investigated in this paper. The configuration of the antenna contains eight modified PIFA elements deployed at four corners of the smartphone mainboard. The proposed design is operating at 2.6, 3.6, and 5.8 GHz for sub 6 GHz 5G mobile terminals. It offers good characteristics in terms of bandwidth, isolation, and radiation pattern. Due to tri-band and polarization diversity characteristics, the antenna can be considered for multi-mode applications.

Acknowledgment

This work is supported by the European Union's Horizon 2020 research and innovation programme under grant agreement H2020-MSCA-ITN-2016 SECRET-722424.

References

[1] A. Osseiran, *et al*., "Scenarios for 5G mobile and wireless communications: the vision of the METIS project," *IEEE Commun. Mag.*, vol. 52, pp.26-35, 2014.

[2] J. G. Andrews *et al.,* "What will 5G be?," *IEEE J. Sel. Areas Commun.,* vol. 32, pp. 1065–1082, 2014.

[3] N. Ojaroudiparchin, *et al*., "Design of Vivaldi antenna array with end-fire beam steering function for 5G mobile terminals", TELFOR 2015, Belgrade, Serbia, pp. 587–590, November 2015.

[4] H.H. Yang,; Y.Q.S. Quel, "Massive MIMO meet small cell. *SpringerBriefs in Electrical and Computer Engineering*, 2017. DOI 10.1007/978-3-319-43715-6_2.

[5] N. Parchin, *et al.,* "UWB mm-wave antenna array with quasi pmnidirectional beams for 5G handheld devices", *ICUWB 2016,* October 2016, Nanjing, China.

[6] M. Jensen, J. Wallace, "A review of antennas and propagation for MIMO wireless communications," *IEEE Trans. Antennas Propag.,* vol. 52, pp. 2810–2824, 2004.

[7] Z. Zhang, "*Antenna Design for Mobile Devices*," Hoboken, NJ, USA: Wiley-IEEE Press, 2011.

[8] N. O. Parchin, *et al.,* "Eight-element dual-polarized MIMO slot antenna system for 5G smartphone applications," *IEEE Access*, vol. 9, pp.15612-15622, 2019.

[9] M. Abdullah, *et al.*, "Eight-element antenna array at 3.5GHz for MIMO wireless application," *PIER C,* vol. 78, pp. 209-217, 2017.

[10] N. O. Parchin, *et al.,* "Dual-polarized MIMO antenna array design using miniaturized self-complementary structures for 5G smartphone applications," *EuCAP Conference*, April 2019, Krakow, Poland.

[11] N. O. Parchin *et al.,* "Modified PIFA array design with improved bandwidth and isolation for 5G mobile handsets," *IEEE 2nd 5G World Forum (5GWF)*, Dresden, Germany, 2019.

[12] Y. Li, *et al.,* "High-isolation 3.5-GHz 8-antenna MIMO array using balanced open slot antenna element for 5G smartphones," *IEEE Trans. Antennas Propag.,* 2019, doi:10.1109/TAP.2019.2902751.

[13] N. O. Parchin *et al.,* "Mobile-phone antenna array with diamond-ring slot elements for 5G massive MIMO systems," *Electronics*, vol. 8, pp. 521, 2019.

[14] N. O. Parchin, *et al.*, "8×8 MIMO antenna system with coupled-fed elements for 5G handsets," *The IET Conference on Antennas and Propagation (APC)*, 11-12 November, 2019, Birmingham, UK.

[15] L. Wang, *et al.,* "Compact UWB MIMO antenna With high isolation using fence-type decoupling structure, *IEEE Antennas and Wireless Propagation Letters*, vol. 8, pp.1641 - 1645, 2019.

[16] P. Salonen, *et al.*, "A small planar inverted-F antenna for wearable applications", *IEEE International Symposium on Wearable Computers*, pp. 96- 100, 1999.

[17] N. Ojaroudi, *et al.*, "An omnidirectional PIFA for downlink and uplink satellite applications in C-band," *Microwave and Optical Technology Letters*, vol. 56, pp. 2684-2686, 2014.

[18] N. Ojaroudi, H. Ojaroudi, and N. Ghadimi, "Quad-band planar inverted-F antenna (PIFA) for wireless communication systems," *Progress In Electromagnetics Research Letters*, vol. 45, pp. 51-56, 2014.

[19] *CST Microwave Studio*, ver. 2017, CST, Framingham, MA, USA, 2017.

[20] N. Ojaroudi, "Design of microstrip antenna for 2.4/5.8 GHz RFID applications," *German Microwave Conference*, GeMic 2014, RWTH Aachen University, Germany, March 10-12, 2014.

[21] A. Valizade, *et al.*, "Band-notch slot antenna with enhanced bandwidth by using Ω-shaped strips protruded inside rectangular slots for UWB applications," ACES Journal, vol. 27, pp. 816–822, 2012.

[22] N. Ojaroudi, "Circular microstrip antenna with dual band-stop performance for ultra-wideband systems," *Microw. Opt. Technol. Lett.*, vol. 56, pp. 2095-2098, 2014.

[23] N. Ojaroudi, and N. Ghadimi, "Design of CPW-fed slot antenna for MIMO system applications," *Microw. Opt. Technol. Lett.,* vol. 56, pp. 1278–1281, 2014.

[24] N. Ojaroudiparchin, M. Shen, and G. F. Pedersen, "End-fire phased array 5G antenna design using leaf-shaped bow-tie elements for 28/38 GHz MIMO applications," *ICUWB 2016*, Nanjing, China, Oct. 16-19, 2016.

[25] N. Ojaroudiparchin, M. Shen, and G. F. Pedersen, "Multi-layer 5G mobile phone antenna for multi-user MIMO communications," *Telecommunications Forum* (*TELFOR 2015)*, November 2015, Serbia.

[26] J. Mazloum, *et al.*, "Compact triple-band S-shaped monopole diversity antenna for MIMO applications," *Applied Computational Electromagnetics Society (ACES) Journal*, vol. 28, pp. 975-980, 2015.

[27] A. Kamalvand, *et al.*, "Omni-directional/multi-resonance CPW-fed small slot antenna for UWB applications," *ACES Journal*, vol. 28, pp. 829-835, 2013.

[28] Y. Al-Yasir, *et al.*, "A new polarization-reconfigurable antenna for 5G applications," *Electronics*, vol. 7, pp. 1-11, 2018.

[29] N. O. Parchin *et al.,* "Frequency reconfigurable sntenna array with compact end-fire radiators for 4G/5G mobile handsets," *IEEE 2nd 5G World Forum (5GWF)*, Dresden, Germany, 2019.

[30] M.S. Sharawi, "*Printed MIMO Antenna Engineering*," Artech House, Norwood, MA, USA, 2014.